# Chemiluminescent Detection of Enzymatically Produced Hydrogen Sulfide: Substrate Hydrogen Bonding Influences Selectivity for H₂S over Biological Thiols

T. Spencer Bailey and Michael D. Pluth*

Department of Chemistry and Biochemistry, Institute of Molecular Biology, University of Oregon, Eugene, Oregon 97403-1253, United States

Ⓢ *Supporting Information*

ABSTRACT: Hydrogen sulfide (H_2S) is now recognized as an important biological regulator and signaling agent that is active in many physiological processes and diseases. Understanding the important roles of this emerging signaling molecule has remained challenging, in part due to the limited methods available for detecting endogenous H_2S. Here we report two reaction-based ChemiLuminescent Sulfide Sensors, CLSS-1 and CLSS-2, with strong luminescence responses toward H_2S (128- and 48-fold, respectively) and H_2S detection limits (0.7 ± 0.3, 4.6 ± 2.0 μM, respectively) compatible with biological H_2S levels. CLSS-2 is highly selective for H_2S over other reactive sulfur, nitrogen, and oxygen species (RSONS) including GSH, Cys, Hcy, $S_2O_3^{2-}$, NO_2^-, HNO, $ONOO^-$, and NO. Despite its similar chemical structure, CLSS-1 displays lower selectivity toward amino acid-

chemiluminescent H₂S response

derived thiols than CLSS-2. The origin of this differential selectivity was investigated using both computational DFT studies and NMR experiments. Our results suggest a model in which amino acid binding to the hydrazide moiety of the luminol-derived probes provides differential access to the reactive azide in CLSS-1 and CLSS-2, thus eroding the selectivity of CLSS-1 for H_2S over Cys and GSH. On the basis of its high selectivity for H_2S, we used CLSS-2 to detect enzymatically produced H_2S from isolated cystathionine γ-lyase (CSE) enzymes ($p < 0.001$) and also from C6 cells expressing CSE ($p < 0.001$). CLSS-2 can readily differentiate between H_2S production in active CSE and CSE inhibited with β-cyanoalanine (BCA) in both isolated CSE enzymes ($p < 0.005$) and in C6 cells ($p < 0.005$). In addition to providing a highly sensitive and selective reaction-based tool for chemiluminescent H_2S detection and quantification, the insights into substrate−probe interactions controlling the selectivity for H_2S over biologically relevant thiols may guide the design of other selective H_2S detection scaffolds.
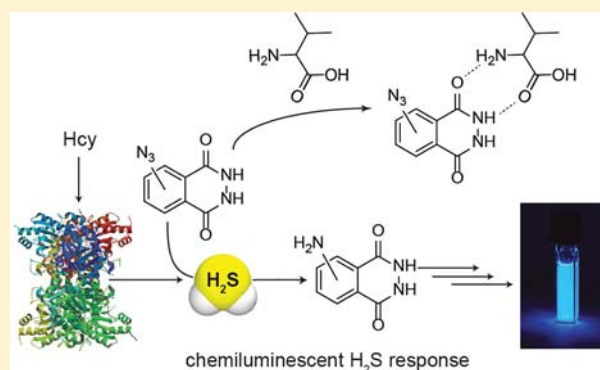
INTRODUCTION

Hydrogen sulfide (H_2S), although generally known for its toxicity and characteristic odor, is now recognized as an important signaling molecule with diverse biological roles. Since the initial studies in 1996 showing that H_2S facilitates hippocampal long-term potentiation (LTP),[1] the discovered biological roles of H_2S have grown rapidly to range from roles in angiogenesis to wound healing.[2−5] In mammals, H_2S production is derived primarily from three enzymes: cystathionine γ-lyase (CSE), cystathionine-β-synthase (CBS), and 3-mercaptopyruvate sulfurtransferase (3-MST).[2] The widespread but differential expression of these enzymes in different tissues suggests a broad importance and significance of H_2S in the cardiovascular, circulatory, respiratory, urinary, and nervous systems. Abnormal H_2S regulation, however, has been associated with hypertension[6] and diabetes,[7] as well as various diseases of mental deficiency including Down's syndrome[8] and Alzheimer's disease.[9] In addition to the pathophysiological conditions associated with H_2S misregulation, H_2S can also act on specific cellular targets, including heme proteins,[10] cysteine

residues on K_{ATP} channels,[11] nitric oxide,[12] and other emerging targets.

As new biological functions of H_2S continue to emerge, new biocompatible tools to monitor H_2S are needed. The primary focus of our research program is aimed at overcoming the limitations of current H_2S detection methods to develop new chemical tools to study the multifaceted roles of H_2S in biology. Traditional methods of H_2S detection, including sulfide-selective electrodes, gas chromatography, or the methylene blue assay, are often limited by poor compatibility with live cells, limited temporal resolution, or extensive sample preparation requirements.[13−15] Recently, reaction-based methods for H_2S detection have emerged, which typically offer higher spatiotemporal resolution and greater live-cell compatibility than traditional detection methods. These reaction-based methods have used H_2S as a nucleophile to attack activated electrophiles[16−20] or precipitate metal salts[21] or as a reductant

to reduce azide or nitro groups on masked fluorophores.[22−25] Recent advances in H_2S detecting probes have focused on probes localized to specific cellular locales in order to report H_2S in specific organelles,[26,27] proteins,[28] and cellular environments.[29] These recently developed probes have expanded the toolbox available to scientists for studying the important and emerging roles of H_2S in biology.

A major challenge for all developed methodologies is effectively differentiating H_2S from the orders of magnitude larger concentrations of cellular GSH. Although azide-based H_2S probes generally show good selectivity for H_2S over other thiols,[30] this selectivity remains generally empirical with little understanding of the design principles required to modulate selectivity. For example, 7-azidocoumarin exhibits excellent (~30-fold) selectivity for 100 μM H_2S over 1 mM cysteine or GSH,[31] whereas 3-azidocoumarin exhibits only 2-fold selectivity for H_2S over 100 μM cysteine or GSH.[32] A second challenge, which complicates azide-based H_2S detection methods, is the inherent photosensitivity of aryl azides. This photosensitivity is generally not problematic for routine detection, but use of higher-powered excitation sources associated with confocal microscopy or HPLC detectors, or the extended excitation of azide-containing fluorophores, may complicate accurate detection. Although azide-based H_2S probes have been used in combination with epifluorescent and confocal microscopy, we have demonstrated that continuous exposure of prototypical azide-containing H_2S probes, such DNS-Az,[24] HSN2,[23] or C-7Az,[31] results in probe photoactivation within minutes (Figure S1, Supporting Information).

One potential solution to this current limitation is to develop a chemiluminescent platform for H_2S detection. Because chemiluminescence does not require an excitation source, there is little chance for photodegredation of the sensing platform. Additionally, because biological materials typically do not spontaneously emit light, chemiluminescent detection methods offer high signal-to-noise ratios. Chemiluminescence is a well-studied analytical tool, capable of producing quantitative data used extensively in immunoassays[33,34] and in chromatography.[35−37] Although the preparation of new chemiluminescent or bioluminescent molecules is an active area of research,[38,39] chemiluminescent detection methods for small molecules remain greatly underexplored. Examples of reaction-based small-molecule chemiluminescent detection have primarily focused on the bioluminescent detection of reactive oxygen species such as H_2O_2.[40−42] Although chemiluminescent thiol detection methods have been reported, these methods typically have low selectivity for a specific thiol and measure the decrease in signal caused by reaction of the analyte with either the luminescent catalyst[43] or the oxidant.[37] On the basis of the opportunity to both expand the palette of chemiluminescent detection methods available for small-molecule biological analytes and overcome current limitations of H_2S-detection platforms, we report here the development of a chemiluminescent platform for H_2S detection. In addition to overcoming the excitation-derived photoactivation common for H_2S fluorescent probes, the developed manifold is used to also present insight, supported by experimental and theoretical underpinnings, into substrate−probe interactions dictating the selectivity for H_2S over other biologically relevant thiols.

■ RESULTS AND DISCUSSION

Probe Design and Response. We envisioned that a chemiluminescent H_2S reporter could be developed by combining H_2S-mediated azide reduction with a luminol-derived sensing platform (Scheme 1). Luminol chemilumines-

Scheme 1. Reduction of a Luminol Azide with H_2S Generates the Parent Luminol Amine. Subsequent Reaction with H_2O_2/HRP (horseradish peroxidase) Generates Chemiluminescence
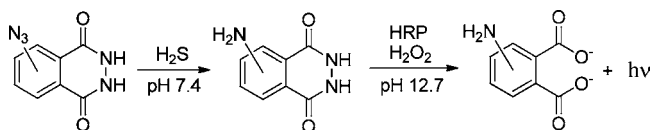
cence results from oxidation of the phthalhydrazide moiety, typically using H_2O_2 as an oxidant, horseradish peroxidase (HRP) as a catalyst to ensure high reproducibility, and an enhancer, such as p-iodophenol, to enhance the chemiluminescence brightness and lifetime.[44,45] Luminol oxidation proceeds through a transient singlet carbonyl species that decomposes to the phthalate product with concomitant N_2 extrusion and photon emission centered at 425 nm.[46] Because derivatizing the luminol amine group to contain electron-withdrawing moieties, such as nitro[47] or acyl[48,49] groups, significantly reduces chemiluminescence, we reasoned that replacement of the amine with an azide would result in a nonchemiluminescent compound. This azide-protected luminol scaffold could then be selectively unmasked by H_2S to generate free luminol and subsequently trigger a large increase in chemiluminescence. On the basis of these considerations, we designed two chemiluminescent sulfide sensors, CLSS-1 and CLSS-2, by converting the amine of luminol and isoluminol to the corresponding azide. CLSS-1 and CLSS-2 are rare examples of reaction-based chemiluminescent probes and, to the best of our knowledge, represent the first example of reaction-based chemiluminescent probes for biological H_2S.

Both luminol and isoluminol can be converted cleanly to their corresponding azides by treatment with tert-butyl nitrite (t-BuONO) and azidotrimethylsilane (TMS-N_3) in DMSO (Scheme 2). Monitoring the reaction of luminol azide (CLSS-

Scheme 2. Synthesis of CLSS-1 and CLSS-2

ortho: luminol
meta: isoluminol

ortho: **CLSS-1** (86%)
meta: **CLSS-2** (83%)
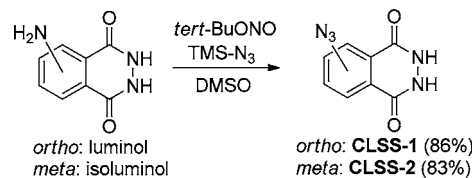
1) or isoluminol azide (CLSS-2) with H_2S by ^1H NMR spectroscopy confirmed clean conversion of each azide to the corresponding amine (Figures S4 and S5, Supporting Information). In the absence of H_2S, treatment of CLSS-1 and CLSS-2 with HRP and H_2O_2 did not generate a chemiluminescent response. By contrast, H_2S-mediated reduction of CLSS-1 or CLSS-2 followed by treatment with HRP and H_2O_2 generates a robust chemiluminescent response which, depending on the concentration, can be monitored spectroscopically or by the naked eye (Figure 1).

Following the H_2S-derived chemiluminescent response of both CLSS-1 and CLSS-2, we determined the detection limit of each probe for H_2S. After incubating each probe for 1 h with different H_2S concentrations, we measured the chemilumines-
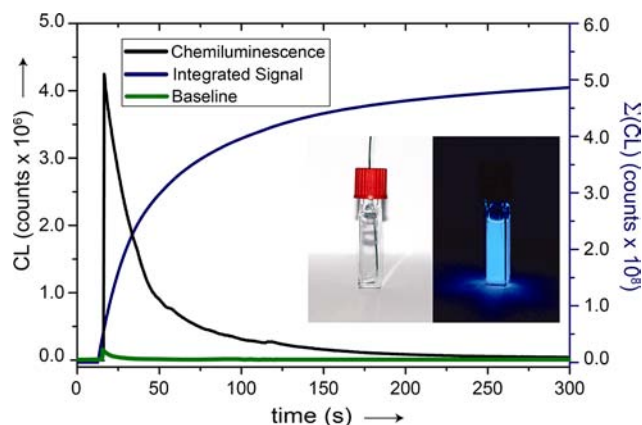
Figure 1. Chemiluminescent response of 50 μM CLSS-1 after incubation with 33 equiv of H_2S. Visual detection (inset) at 10× concentration, 5 s camera exposure. Samples were incubated for 60 min in pH 7.4 PIPES buffer at 37 °C prior to analysis.

cent response after treatment with H_2O_2/HRP using *p*-iodophenol as an enhancer. A linear chemiluminescent response was observed for both CLSS-1 and CLSS-2 (Figure 2), thereby demonstrating the ability of each probe to quantify
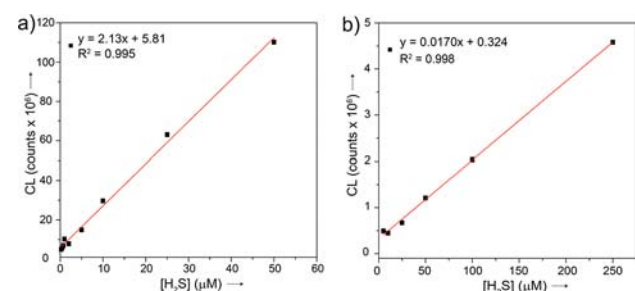
Figure 2. Concentration dependence of H_2S on the luminescence of (a) CLSS-1 and (b) CLSS-2. Values obtained are the background-corrected integrated emission at λ_{em} = 425 nm and represent the average of at least three replicates. Samples were incubated for 60 min in pH 7.4 PIPES buffer at 37 °C prior to analysis.

different H_2S concentrations. On the basis of the concentration-dependent H_2S response and the instrumental background measurements, we determined the H_2S detection limit (3σ) of CLSS-1 and CLSS-2 to be 0.7 ± 0.3 μM and 4.6 ± 2.0 μM, respectively. Although the total brightness of CLSS-2 is lower than that of CLSS-1, both of the detection limits are below the reported range of H_2S concentrations (20−100 μM) found in mammalian blood.[50−53] The effective concentration range where CLSS-1 and CLSS-2 have been shown to accurately detect H_2S (Figure 2) cover this entire range, highlighting the sensitivity and versatility of the developed sensing platform.

Selectivity for H_2S. We next tested the response of CLSS-1 and CLSS-2 to biologically relevant reactive sulfur, oxygen, and nitrogen species (RSONS). We first tested the selectivity of CLSS-1 for H_2S by addition of 33 equiv of cysteine (Cys), homocysteine (Hcy), *N*-acetylcysteine (NAC), reduced gluta-thione (GSH), thiosulfate ($S_2O_3^{2-}$), sulfate (SO_4^{2-}), nitric oxide (NO), nitroxyl (HNO), and nitrite (NO_2^-) (Figure 3). On the basis of previous reports using H_2S as a reductant for azides,[30] we expected that CLSS-1 would be highly selective for H_2S over RSONS including biologically relevant thiols. Much
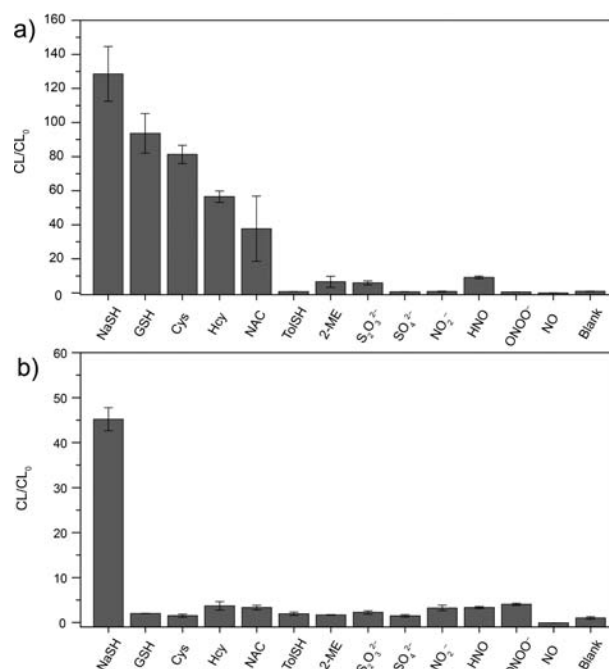

Figure 3. Selectivity of (a) CLSS-1 and (b) CLSS-2 with reactive oxygen, nitrogen, and sulfur species. Conditions: 50 μM probe, 33 equiv of RSONS, incubated 1 h at 37 °C. The reported intensities are background-corrected, represent the integrated luminescence (λ_{em} = 425 nm), and are the average of at least three replicates. Error bars represent ± SE.

to our surprise, although CLSS-1 showed a 128-fold turn on for H_2S and high selectivity for H_2S over oxygen and nitrogen reactive species, poor selectivity was observed with cysteine-derived reductants. Because CLSS-1 did not react with other reductants, such as HNO, we hypothesized that the observed chemiluminescent response from cysteine-derived thiols could be due to hydrogen bonding of the amino acid substrate to the luminol hydrazide moiety (Figure 5). Such hydrogen bonding would increase the effective thiol concentration near the azide of CLSS-1, orient the thiol toward attack on the azide (vide infra), and subsequently erode the selectivity for H_2S over thiols.[54] To test this theory experimentally, CLSS-1 was treated with *p*-toluenethiol (TolSH), which lacks an amino acid moiety to hydrogen bond with the luminol hydrazide. Consistent with our hypothesis, TolSH did not generate a chemiluminescent response from CLSS-1. Furthermore, CLSS-1 was also treated with 2-mercaptoethanol (2-ME), an alkyl thiol with a reduction potential (−0.26 V)[55] similar to that of cysteine (−0.22 V),[56] and no chemiluminescent response was observed (Figure 3). On the basis of these results, we expected that moving the azide from the ortho to meta ring position would increase the selectivity for H_2S over amino acid-derived thiols because of the increased distance from the hydrazide moiety to the azide. Consistent with our hypothesis, CLSS-2 showed a 45-fold turn on for H_2S and high selectivity for H_2S over other RSONS (Figure 3b) including other reductants, such as TolSH, 2-ME, or HNO.[57] Similarly, treatment of CLSS-2 with 20 mM Cys does not result in a chemiluminescent response. These results demonstrate the efficacy of CLSS-2 as a selective chemilumi-nescent H_2S detector.

Understanding the Differential Reactivity of CLSS-1 and CLSS-2. To further understand the reactivity differences between CLSS-1 and CLSS-2, and to substantiate our

hydrogen-bonding model, we performed DFT calculations at the B3LYP/6-311++G(d,p) level of theory using the IEFPCM water solvation model for each probe as well as cysteine-coordinated adducts. We chose cysteine as a model amino acid for these studies because of its differential reactivity toward CLSS-1 and CLSS-2 and also fewer available rotational and protonation states by comparison to GSH. To confirm that changes in the frontier orbital landscape of CLSS-1 and CLSS-2 were not responsible for the differential reactivity between the two probes, we calculated the HOMO and LUMO of CLSS-1 and CLSS-2. For both probes, the HOMO and LUMO are localized exclusively on the azide, suggesting that orbital differences or LUMO accessibility is not the source of the differential reactivity between CLSS-1 and CLSS-2 (Figure 4).
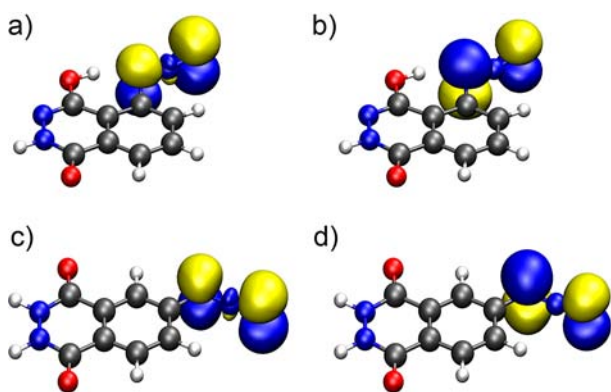
Figure 4. Frontier molecular orbitals of CLSS-1 and CLSS-2. (a) CLSS-1 HOMO, (b) CLSS-1 LUMO, (c) CLSS-2 HOMO, (d) CLSS-2 LUMO.

To investigate whether amino acid-derived thiol interaction with to the hydrazide moiety could contribute to the lower selectivity of CLSS-1, we optimized the geometry of the cysteine-bound adducts of both CLSS-1 and CLSS-2. In all cases all luminol tautomers and cysteine protonation states were investigated to ensure that a broad potential energy surface was surveyed during the optimizations. The optimized geometry of the CLSS-1/Cys adduct corresponded to a geometry in which the cysteine is hydrogen-bonded to the hydrazide moiety and the cysteine thiol is situated 2.67 Å away from the azide nitrogen, suggesting a hydrogen bond between the SH and the azide group (Figure 5). This hydrogen bond distance is consistent with crystallographically characterized hydrogen bonds between N—H or O—H groups and the terminal nitrogen of azides.[58−61] By contrast, the optimized
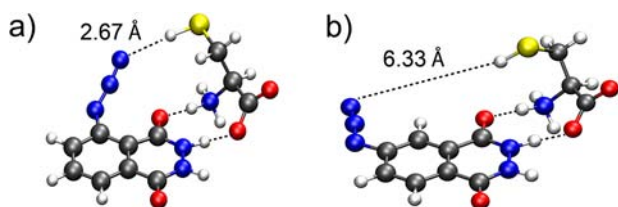
Figure 5. The calculated CLSS-1/Cys structure (a) is consistent with a weak hydrogen bond between the terminal nitrogen of the azide and the cysteine thiol. For CLSS-2/Cys (b), the distance between the azide and the cysteine thiol group is too large for a hydrogen bonding interaction. Geometries were optimized using Gaussian 09, B3LYP/6-311++G(d,p), using the IEPCM water solvation model.

geometry of the CLSS-2/Cys reveals that the thiol group from the cysteine is too far away from the azide to result in a favorable hydrogen bonding interaction. These structures corresponding to the energy minima of the CLSS-1/Cys and CLSS-2/Cys adducts are consistent with our hypothesis that amino acid hydrogen bonding to the luminol hydrazide dictates the observed selectivity differences for the two probes toward thiol-containing amino acids.

To further understand the favorability of forming each adduct, we also compared the energies of the hydrogen-bonded adducts to other species likely present in solution. Because phthalhydrazides typically adopt a trimeric form in the solid state,[62] we also optimized the hydrogen-bonded trimer for both CLSS-1 and CLSS-2. For CLSS-1, the CLSS-1/Cys adduct, in which the amino acid moiety was bound to the hydrazide and the thiol group was hydrogen bonded to the terminal nitrogen of the azide, was the global energy minimum (Figure 6a). This conformation is 7.4 kcal/mol more stable than isolated CLSS-1 and cysteine, 1.5 kcal/mol more stable than the CLSS-1/Cys adduct minimum without an SH/N$_3$ hydrogen bond, and 0.7 kcal/mol more stable than the CLSS-1 trimer. By contrast, the structure of CLSS-2 does not allow for SH/N$_3$ hydrogen bonding during cysteine coordination because of the large interatomic distance between the thiol and the azide (Figure 6b). In this case, the CLSS-2/Cys adduct is 0.5 kcal/mol less stable than the CLSS-2 trimer. Taken together, the results of the computational studies of CLSS-1 and CLSS-2 are consistent with the hypothesis that hydrogen bonding of cysteine to the hydrazide and azide erodes the selectivity of CLSS-1. Not only do these results help explain the observed selectivity, but they also provide valuable design strategies for developing future generations of highly selective H$_2$S probes.

In addition to computational evidence for our hydrogen-bonding hypothesis, we also performed NMR titrations of CLSS-1 and CLSS-2 with different amino acids to further validate our model with solution data. We chose to use serine as a model amino acid because cysteine quickly reduces CLSS-1 under typical experimental conditions. Furthermore, the alcohol side chain of serine maintains a hydrogen bond donor but, unlike cysteine, is redox inactive. All ^{1}H NMR titrations were performed in DMSO to ensure complete solubility of all components and to provide a hydrogen-bond disrupting environment similar to water. Similarly, to model the protonation state of the amino acids in water, and also to ensure complete solubility through the course of the titration, we prepared the tetrabutylammonium salts of each amino acid. By titrating tetrabutylammonium serine (TBA-Ser) into a solution of CLSS-1 and CLSS-2, striking changes in the aromatic region of the NMR spectra were observed, consistent with amino acid binding to the hydrazide moiety (Figure 7).

Control experiments to investigate dilution effects on CLSS-1 and CLSS-2, as well as self-association studies of TBA-Ser, did not result in shifts in the aromatic region of the spectrum. These changes in the ^{1}H NMR shifts were fit to a 1:1 binding model using the Thordarson fitting program[63] to afford binding affinities of 380 ± 80 M^{-1} and 260 ± 60 M^{-1} for CLSS-1/TBA-Ser and CLSS-2/TBA-Ser, respectively (Table 1). The slightly tighter binding of TBA-Ser to CLSS-1 over CLSS-2 is consistent with the computational studies and the proposed hydrogen bonding model.

We also performed ^{1}H NMR titrations with tetrabutylammonium valine (TBA-Val) as a second model system in which the side chain of the amino acid cannot hydrogen bond to the
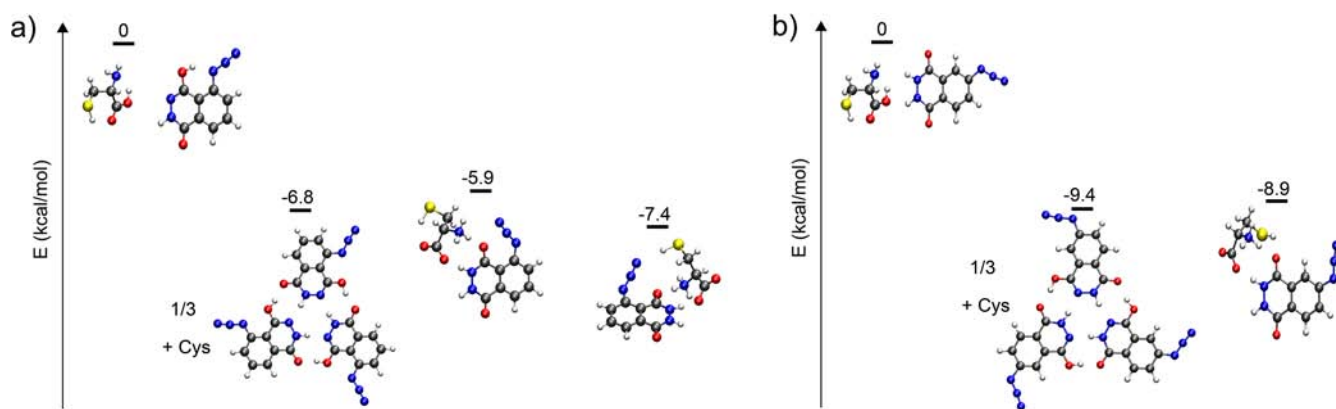
Figure 6. Energetic landscape of (a) CLSS-1 and (b) CLSS-2 binding to cysteine. For CLSS-1, the minimum energy state corresponds to the CLSS-1/Cys adduct with a N_3/SH hydrogen bond.
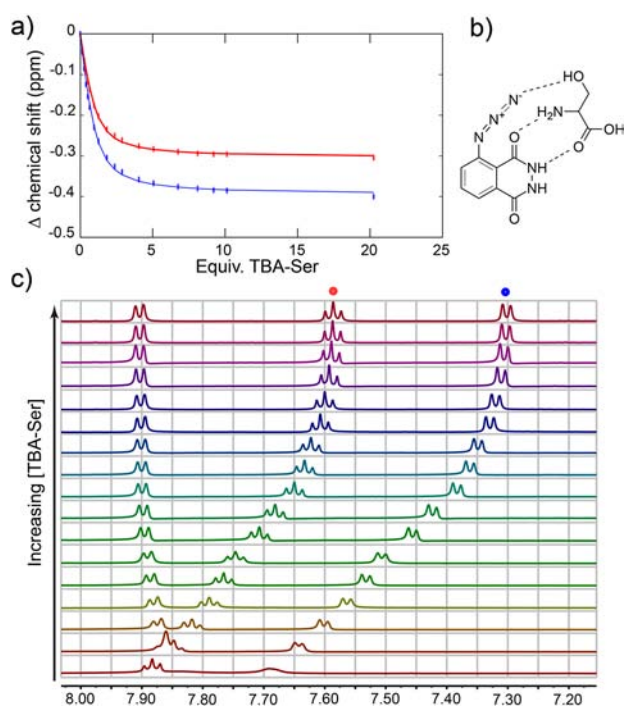
Figure 7. Representative titration data for TBA-Ser with CLSS-1. (a) Nonlinear fitting of aromatic chemical shifts based on a 1:1 binding model, (b) proposed binding interaction, and (c) stacked ^1H NMR spectra showing the changes in the aromatic region of CLSS-1 during the course of the titration.

Table 1. Binding Affinities for CLSS-1 and CLSS-2 with Model Amino Acids[a]

|	binding affinities (M^{-1})	
	CLSS-1	CLSS-2
TBA-Ser	380 ± 80	260 ± 60
TBA-Val	3640 ± 270	3780 ± 370

[a]Conditions: 10.0 mM probe, 0−200 mM amino acid, DMSO-d_6, 25.0 °C. Each value represents the average of three independent titrations.

azide. As observed with TBA-Ser, TBA-Val binds to both CLSS-1 and CLSS-2 in a 1:1 stoichiometry with binding affinities of 3640 ± 270 M^{-1} and 3780 ± 370 M^{-1} for CLSS-1 and CLSS-2, respectively. The binding affinities measured for TBA-Val are larger than for TBA-Ser (Table 1), which is

consistent with the reduced internal competition for intramolecular hydrogen bonding sites in valine. On the basis of these titration data, and the lower hydrogen bonding ability of thiols by comparison to alcohols, we expect the binding affinity of cysteine for CLSS-1 and CLSS-2 to be between the measured values for serine and valine. Under the general experimental conditions used to measure the selectivity date, a 10^3-10^4 M^{-1} binding affinity between Cys/CLSS-1 would result in significant generation of the Cys/CLSS-1 adduct, which is consistent with the observed erosion in selectivity. In total, the NMR titration data are consistent with our model of amino acids binding to the luminol scaffold, which in turn, is consistent with the observed lower selectivity of CLSS-1 than CLSS-2 for H_2S over amino acid-containing thiols.

Chemiluminescent Detection of Enzymatically Produced H_2S. Having determined that CLSS-2 is highly selective for H_2S over other RSONS, we next demonstrated the ability of CLSS-2 to detect enzymatically produced H_2S by using isolated and purified cystathionine γ-lyase (CSE). CSE is a PLP-dependent enzyme that converts Hcy or Cys to H_2S[64] and can be inhibited by β-cyano-L-alanine (BCA).[65] Control experiments measuring the response of CLSS-2 to Hcy, BCA, and the reaction byproducts pyruvate (Pyr) and NH_3 all showed statistically significant lower ($p < 0.005$) chemiluminescent responses (Figure 8, white bars). Similarly, incubation of CLSS-2 with CSE in the absence of substrate showed no response. Introduction of the Hcy substrate to CSE, however, resulted in a robust response by comparison to CSE alone ($p < 0.001$) or CSE and Hcy inhibited with BCA ($p < 0.005$) (Figure 8, light gray bars). Furthermore, quantification of the H_2S produced from the CSE/Hcy system using the chemiluminescent response curve in Figure 2a is in agreement with the expected concentrations based on known CSE kinetic parameters.[66] Taken together, these results demonstrate the ability of CLSS-2 to detect and quantify enzymatically produced H_2S from CSE and also differentiate between inhibited and uninhibited enzymes.

We next demonstrated the ability of CLSS-2 to detect and quantify endogenously produced H_2S in C6 cells. C6 cells express CSE and produce H_2S endogenously,[67] thereby providing an ideal platform to demonstrate H_2S detection in the presence of other active biological processes. Incubation of CLSS-2 with C6 cell lysates lacking CSE substrates resulted in minimal luminescent response (Figure 8, dark gray), consistent with limited cellular H_2S production. This result confirmed that other biological species in the cellular milieu do not activate
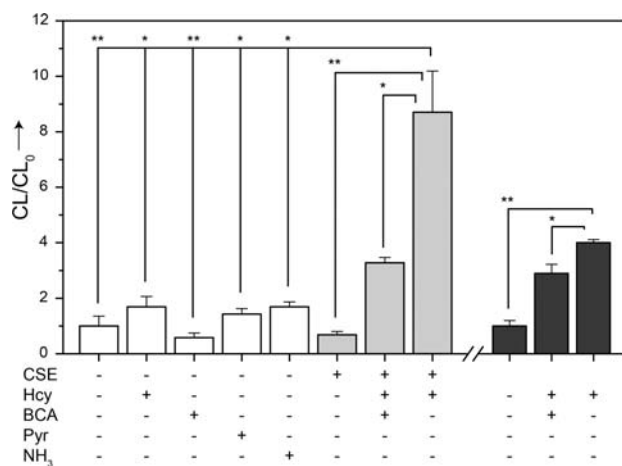
Figure 8. Detection of CSE-produced H_2S using CLSS-2. Conditions: Absence of enzyme (white), 10 μg CSE (light gray), 20 mM Hcy, 20 mM BCA, 25 μM pyruvate, 25 μM NH_3; incubated in 3.0 mL buffer at 37 °C for 48 h prior to detection with 50 μM CLSS-2. Comparison with C6 cell lysates containing 2×10^6 cells (dark gray). Each data point represents the mean $\pm$ SE derived from at least three independent experiments; * indicates $p < 0.005$ and ** indicates $p < 0.001$.

CLSS-2. By contrast, addition of Hcy as a CSE substrate significantly increased luminescence ($p < 0.001$) by comparison to lysates lacking substrate, signifying that CSE present in the cell lysates produced sufficient H_2S to be detected by CLSS-2. Furthermore, addition of Hcy and BCA abrogated the luminescent response ($p < 0.005$), which is consistent with CSE inhibition. These results build upon the isolated CSE experiments and demonstrate that CLSS-2 can detect endogenously produced H_2S even in the presence of other biological species.

CONCLUSIONS

We have prepared two chemiluminescent probes for H_2S capable of detecting at physiologically relevant levels of H_2S. Not only are these probes the first example of reaction-based chemiluminescent probes for H_2S, but they also offer insight into new strategies to separate the reactivity of H_2S from other biological thiols based on hydrogen bonding. In addition to detecting exogenous H_2S, we demonstrated that CLSS-2 can detect enzymatically produced H_2S from both isolated CSE enzymes and also from C6 cell lysates and can also differentiate inhibited and native states of the enzyme. We anticipate that the chemical tools outlined here, as well as future scaffolds based on the design principles, will contribute to a greater understanding the multifaceted roles of biological H_2S.

EXPERIMENTAL SECTION

Materials and Methods. Synthetic precursors 3-aminophthalhydrazide and 4-aminophthalhydrazide were purchased from TCI and used as received. Tetrabutylammonium amino acid salts (TBA-Ser, TBA-Val),[68] HSN-2,[23] DsN3,[24] and C-7Az[31] were prepared as described in the literature. Deuterated solvents were purchased from Cambridge Isotope Laboratories and used as received. Piperazine-N,N′-bis(2-ethansulfonic acid) (PIPES, Aldrich) and potassium chloride (99.999%, Aldrich) were used to make buffered solutions (50 mM PIPES, 100 mM KCl, pH 7.4) with Millipore water. Buffered solutions were degassed by vigorous sparging with N_2 and stored in an inert atmosphere glovebox. Anhydrous sodium hydrogen sulfide (NaSH) was purchased from Strem Chemicals and handled under

nitrogen. S-Nitroso-N-acetyl-DL-penicillamine (SNAP), sodium peroxynitrite (NaO_2NO), and Angeli's salt (NaN_2O_3) were purchased from Cayman Chemical and stored either at −30 °C or −80 °C prior to use. L-Cysteine, N-acetyl-L-cysteine, and DL-homocysteine were purchased from TCI. Reduced glutathione was purchased from Aldrich. Stock solutions of the reactive species were prepared in either buffer or DMSO under nitrogen immediately prior to use and were introduced into buffered solutions with a syringe. Note: Although CLSS-1 and CLSS-2 are not air-sensitive, some of the reactive sulfur, oxygen, and nitrogen species, including H_2S, are known to react with oxygen. To ensure accurate measurements and to prevent decomposition of potentially reactive species, all experiments were performed under an inert atmosphere unless otherwise indicated. Both CLSS-1 and CLSS-2 react with H_2S under aerobic conditions to provide equivalent results as under anaerobic conditions. Stock solutions of the chemiluminescent probes (10 mM) were prepared in DMSO and stored below −20 °C until immediately prior to use. In all spectroscopic experiments, the final concentration of DMSO was less than 0.5% of the total buffer volume.

Spectroscopic Methods. NMR spectra were acquired on a Brüker Avance-III-HD 600 spectrometer with a Prodigy multinuclear broadband CryoProbe at 25.0 °C. Chemical shifts are reported in parts per million (δ) and are referenced to residual protic solvent resonances. The following abbreviations are used in describing NMR couplings: (s) singlet, (d) doublet, (b) broad, and (m) multiplet. IR spectra were measured on a Thermo Scientific Nicolet 6700 RT-IR using an ATR attachment. Chemiluminescence measurements were obtained on a Photon Technology International Quanta Master 40 spectrofluorimeter equipped with a Quantum Northwest TLC-50 temperature controller at 37.0 $\pm$ 0.05 °C. All chemiluminescent measurements were made under an inert atmosphere in septum-sealed cuvettes obtained from Starna Scientific and were repeated at least in triplicate. High resolution mass spectrometry (HRMS) measurements were performed by the Biomolecular Mass Spectrometry Core of the Environmental Health Sciences Core Center at Oregon State University. Melting points were obtained using a Laboratory Devices Mel-Temp and are reported uncorrected.

General Procedure for NMR Titrations. A septum-sealed NMR tube was charged with either CLSS-1 or CLSS-2 (10 mM in 300 μL of DMSO-d_6) under N_2-atmosphere and aliquots of a DMSO-d_6 solution containing 200 mM amino acid mixed with 10 mM of the probe were added using a syringe. The chemical shifts of the aromatic proton resonances were tracked, and the data were fit to a 1:1 binding model.[63]

Computational Details. Calculations were performed using the Gaussian 09 software package[69] with the GaussView graphical user interface.[70] Graphical representations were produced using VMD v1.9.[71] Geometry optimizations and unscaled frequency calculations were carried out at the B3LYP/6-311++G(d,p) level of theory using the IEF-PCM solvation model for water. Frequency calculations were performed on all converged structures to confirm that they corresponded to local minima. Calculated enthalpies are reported as zero-point corrected enthalpies. Initial structures for geometry optimizations were screened as follows: Each luminol tautomer was optimized starting with multiple azide orientations. For cysteine–luminol adducts, each luminol tautomer was optimized with the RCO_2H/RNH_2 and RCO_2^-/RNH_3^+ protonation states, multiple azide orientations, and multiple cysteine dihedral angles. In all cases, the lowest energy conformer/tautomer was used to compare the relative energetics of the calculated species.

General Procedure for Luminescence Measurements. In a septum-sealed cuvette, a solution of the probe (50 μM) and the desired reactive species was incubated in 3.0 mL of PIPES buffer (50 mM PIPES, 100 mM KCl, pH 7.4) for 60 min at 37.0 °C After incubation, 40 μL of 6 M NaOH was added to increase the pH to 12.7, an optimal level for luminol chemiluminescence, and also assures complete conversion of any remaining H_2S to sulfate upon addition of H_2O_2.[72] After pH adjustment, 10 μL of 10 U/mL horseradish peroxidase (HRP) with 0.2 μM p-iodophenol was added. A background reading was acquired for 60 s, after which 50 μL of

H_2O_2 (35%) was added. The sample luminosity at 425 nm was integrated for 300 s after H_2O_2 addition. The data reported are the average of at least three independent experiments. Errors are reported as $\pm$ SE, and p-values report the one-way ANOVA values.

General Procedure for Photoactivation Experiments. In a septum-sealed cuvette, a 5 μM solution of each probe in PIPES buffer (50 mM PIPES, 100 mM KCl, pH 7.4) was excited at the absorption maximum of the corresponding amine product for 25 min at 37 °C. The fluorescence signal of each sample was detected at the emission maximum for the unprotected fluorophore with excitation and emission slit widths set at 5 and 1.4 nm, respectively. The normalized data are presented in Figure S1, Supporting Information.

General Procedure for Enzymatically Produced H_2S Luminescence Measurements. In a septum-sealed cuvette, the desired reactive species were incubated in 3.0 mL of PIPES buffer (50 mM PIPES, 100 mM KCl, pH 7.4) at 37.0 °C for 48 h. After initial incubation, 15 μL of 10 mM CLSS-2 in DMSO was added and allowed to react for 60 min. After incubation, 40 μL of 6 M NaOH was added to increase the pH to 12.7, an optimal level for luminol chemiluminescence. After pH adjustment, 10 μL of 10 U/mL horseradish peroxidase (HRP) with 0.2 μM p-iodophenol was added. A background reading was acquired for 60 s, after which 50 μL of H_2O_2 (35%) was added. The sample luminosity at 425 nm was integrated for 40 s after H_2O_2 addition. The data reported are the average of at least three independent experiments.

Cell Culture and Lysing Procedure. C6 cells were obtained from ATCC and cultured in Dulbecco's Modified Eagle Medium (DMEM, Cellgro, MediaTek, Inc.) supplemented with 10% fetal bovine serum (FBS, HyClone), and 1% penicillin/streptomycin. Cells were passed, plated into T-75 flasks containing 10 mL of DMEM, and incubated at 37 °C with 5% CO_2. For luminescence studies, the cells were washed with 1x phosphate-buffered saline (PBS), trypsinized with 5 mL of trypsin, and then centrifuged to form a cell pellet. The cell pellet was resuspended in 5 mL of 1x PBS, and the cells were counted using a Bio RAD TC20 automated cell counter. Cells were centrifuged at 1000 rpm for 5 min at room temperature, placed on ice, and lysed using 100 μL of RIPA buffer (pH 7.5 10 mM Tris-HCl, 150 mM NaCl, 1.0% Nonidet P-40, 0.1% SDS, 0.1% sodium deoxycholate) containing protease inhibitor (PhosSTOP, Roche) for every 2×10^6 cells in the pellet. Luminescence measurements on cell lysates were made using 100 μL of lysate solution (2×10^6 cells per experiment) under ambient atmosphere by following the general procedure for enzymatically produced H_2S outlined above.

Syntheses. *General Procedure for Azidification.* The appropriate aminophthalhydrazide (0.10 g, 0.56 mmol) was dissolved in 5 mL of dry DMSO. After the solution was cooled to 0 °C, 0.10 mL (0.85 mmol) of *tert*-butyl nitrite was added dropwise. The reaction mixture was stirred for 1 h, and then 0.95 mL (0.68 mmol) of trimethylsilyl azide (TMS-N_3) was added. The reaction mixture was allowed to warm to room temperature and was stirred for 1 h. Volatile components of the reaction mixture were then removed under vacuum without heating. The remaining DMSO solution was diluted with 50 mL of 5% dichloromethane in hexanes to yield a precipitate. The precipitate was collected and washed with dichloromethane to afford the desired azide. The spectroscopic parameters of compounds CLSS-1 and CLSS-2, prepared by this method, are tabulated below.

3-Azidophthalhydrazide (CLSS-1). Yield. 95 mg (83%). ^{1}H NMR (600 MHz, DMSO-d_6) δ: 11.52 (b, 2H, NH), 7.87 (m, 2H, ArH), 7.68 (d, J = 7.7 Hz, 1H, ArH). ^{13}C{^{1}H} NMR (150 MHz, DMSO-d_6) δ: 156.0, 152.0, 139.3, 134.0, 128.8, 125.5, 122.2, 119.7. IR (cm^{-1}): 3167, 3013, 1896, 2617, 2191 [$\nu(N_3)$], 2101 [$\nu(N_3)$], 1650, 1611, 1597, 1487, 1454, 1357, 1326, 1290, 1206, 1193, 1180, 1164, 1121, 1067, 1003, 980, 902, 871, 769, 733, 697. Mp: 165 °C (decomp). HRMS-ESI (m/z): [M + H]$^+$ calcd for [$C_8H_6O_2N_5$]$^+$, 204.0521; found 204.0524.

4-Azidophthalhydrazide (CLSS-2). Yield: 100 mg (87%). ^{1}H NMR (600 MHz, DMSO-d_6) δ: 11.57 (s, br, 2H, NH), 8.07 (d, J = 8.5 Hz, 1H, ArH), 7.60 (s, 1H, ArH), 7.57 (dd, J = 8.5, 2.3 Hz, 1H, ArH). ^{13}C{^{1}H} NMR (150 MHz, DMSO-d_6) δ: 154.6, 154.4, 144.4, 133.0, 129.0, 128.1, 124.4, 114.5.; IR (cm^{-1}): 3417 3164, 3008, 2914, 2120 [$\nu(N_3)$], 1662, 1603, 1554, 1496, 1458, 1435, 1405, 1367, 1344, 1290, 1252, 1218, 1172, 1108, 951, 819, 731, 646. Mp: 165 °C (decomp). HRMS-EI (m/z): [M]$^+$ calcd for [$C_8H_5O_2N_5$]$^+$, 203.04433; found 203.04392.

■ ASSOCIATED CONTENT

S **Supporting Information**
Tabulated selectivity data, titration data, photoactivation data, ^{1}H and ^{13}C{^{1}H} NMR spectra, mass spectra, and optimized geometries for DFT calculations. This material is available free of charge via the Internet at http://pubs.acs.org.

■ AUTHOR INFORMATION

Corresponding Author
pluth@uoregon.edu
Notes
The authors declare no competing financial interest.

■ ACKNOWLEDGMENTS

■ REFERENCES

(1) Abe, K.; Kimura, H. *J. Neurosci.* **1996**, *16*, 1066−1071.
(2) Wang, R. *Physiol. Rev.* **2012**, *92*, 791−896.
(3) Whiteman, M.; Moore, P. K. *J. Cell. Mol. Med.* **2009**, *13*, 488−507.
(4) Wallace, J. L.; Dicay, M.; McKnight, W.; Martin, G. R. *FASEB J.* **2007**, *21*, 4070−4076.
(5) Wang, R. *Kidney Int.* **2009**, *76*, 700−704.
(6) Yang, G. D.; Wu, L. Y.; Jiang, B.; Yang, W.; Qi, J. S.; Cao, K.; Meng, Q. H.; Mustafa, A. K.; Mu, W. T.; Zhang, S. M.; Snyder, S. H.; Wang, R. *Science* **2008**, *322*, 587−590.
(7) Wu, L. Y.; Yang, W.; Jia, X. M.; Yang, G. D.; Duridanova, D.; Cao, K.; Wang, R. *Lab. Invest.* **2009**, *89*, 59−67.
(8) Chen, C.-Q.; Xin, H.; Zhu, Y.-Z. *Acta Pharmacol. Sin.* **2007**, *28*, 1709−1716.
(9) Qu, K.; Lee, S. W.; Bian, J. S.; Low, C. M.; Wong, P. T. H. *Neurochem. Int.* **2008**, *52*, 155−165.
(10) Pietri, R.; Roman-Morales, E.; Lopez-Garriga, J. *Antioxid. Redox Signaling* **2011**, *15*, 393−404.
(11) Jiang, B.; Tang, G. H.; Cao, K.; Wu, L. Y.; Wang, R. *Antioxid. Redox Signaling* **2010**, *12*, 1167−1178.
(12) Filipovic, M. R.; Miljkovic, J. L.; Nauser, T.; Royzen, M.; Klos, K.; Shubina, T.; Koppenol, W. H.; Lippard, S. J.; Ivanovic-Burmazovic, I. *J. Am. Chem. Soc.* **2012**, *134*, 12016−12027.
(13) DeLeon, E. R.; Stoy, G. F.; Olson, K. R. *Anal. Biochem.* **2012**, *421*, 203−207.
(14) Fogo, J. K.; Popowsky, M. *Anal. Chem.* **1947**, *21*, 732−734.
(15) Lawrence, N. S.; Davis, J.; Compton, R. G. *Talanta* **2000**, *52*, 771−784.
(16) Qian, Y.; Karpus, J.; Kabil, O.; Zhang, S. Y.; Zhu, H. L.; Banerjee, R.; Zhao, J.; He, C. *Nat. Commun.* **2011**, *2*.
(17) Liu, C. R.; Pan, J.; Li, S.; Zhao, Y.; Wu, L. Y.; Berkman, C. E.; Whorton, A. R.; Xian, M. *Angew. Chem., Int. Ed.* **2011**, *50*, 10327−10329.
(18) Shen, X.; Pattillo, C. B.; Pardue, S.; Bir, S. C.; Wang, R.; Kevil, C. G. *Free Radical Biol. Med.* **2011**, *50*, 1021−1031.
(19) Chen, Y.; Zhu, C.; Yang, Z.; Chen, J.; He, Y.; Jiao, Y.; He, W.; Qiu, L.; Cen, J.; Guo, Z. *Angew. Chem., Int. Ed.* **2013**, *52*, 1688−1691.

(20) Montoya, L. A.; Pearce, T. F.; Hansen, R. J.; Zakharov, L. N.; Pluth, M. D. *J. Org. Chem.* **2013**, *78*, 6550−6557.

(21) Sasakura, K.; Hanaoka, K.; Shibuya, N.; Mikami, Y.; Kimura, Y.; Komatsu, T.; Ueno, T.; Terai, T.; Kimura, H.; Nagano, T. *J. Am. Chem. Soc.* **2011**, *133*, 18003−18005.

(22) Lippert, A. R.; New, E. J.; Chang, C. J. *J. Am. Chem. Soc.* **2011**, *133*, 10078−10080.

(23) Montoya, L. A.; Pluth, M. D. *Chem. Commun.* **2012**, *48*, 4767−4769.

(24) Peng, H.; Cheng, Y.; Dai, C.; King, A. L.; Predmore, B. L.; Lefer, D. J.; Wang, B. *Angew. Chem., Int. Ed.* **2011**, *50*, 9672−9675.

(25) Thorson, M. K.; Majtan, T.; Kraus, J. P.; Barrios, A. M. *Angew. Chem., Int. Ed.* **2013**, *52*, 4641−4644.

(26) Liu, T.; Xu, Z.; Spring, D. R.; Cui, J. *Org. Lett.* **2013**, *15*, 2310−2313.

(27) Bae, S. K.; Heo, C. H.; Choi, D. J.; Sen, D.; Joe, E.-H.; Cho, B. R.; Kim, H. M. *J. Am. Chem. Soc.* **2013**, *135*, 9915−9923.

(28) Chen, S.; Chen, Z.-J.; Ren, W.; Ai, H.-W. *J. Am. Chem. Soc.* **2012**, *134*, 9589−9592.

(29) Lin, V. S.; Lippert, A. R.; Chang, C. J. *Proc. Natl. Acad. Sci. U.S.A.* **2013**, *110*, 7131−7135.

(30) Lin, V. S.; Chang, C. J. *Curr. Opin. Chem. Biol.* **2012**, *16*, 595−601.

(31) Chen, B.; Li, W.; Lv, C.; Zhao, M.; Jin, H.; Jin, H.; Du, J.; Zhang, L.; Tang, X. *Analyst* **2013**, *138*, 946−951.

(32) Li, W.; Sun, W.; Yu, X.; Du, L.; Li, M. *J. Fluoresc.* **2013**, *23*, 181−186.

(33) Williams, E. J.; Campbell, A. K. *Anal. Biochem.* **1986**, *155*, 249−255.

(34) Yuan, H.; Chong, H.; Wang, B.; Zhu, C.; Liu, L.; Yang, Q.; Lv, F.; Wang, S. *J. Am. Chem. Soc.* **2012**, *134*, 13184−13187.

(35) Yan, X. *J. Sep. Sci.* **2006**, *29*, 1931−1945.

(36) Thurbide, K. B.; Aue, W. A. *Spectrochim. Acta, Part B* **2002**, *57*, 843−852.

(37) Garcia, I. L.; Vinas, P.; Gil, J. A. M. *Fresenius J. Anal. Chem.* **1993**, *345*, 723−726.

(38) McCutcheon, D. C.; Paley, M. A.; Steinhardt, R. C.; Prescher, J. A. *J. Am. Chem. Soc.* **2012**, *134*, 7604−7607.

(39) Sun, Y. Q.; Liu, J.; Wang, P.; Zhang, J.; Guo, W. *Angew. Chem., Int. Ed.* **2012**, *51*, 8428−8430.

(40) Van de Bittner, G. C.; Dubikovskaya, E. A.; Bertozzi, C. R.; Chang, C. J. *Proc. Natl. Acad. Sci. U.S.A.* **2010**, *107*, 21316−21321.

(41) Yamaguchi, S.; Kishikawa, N.; Ohyama, K.; Ohba, Y.; Kohno, M.; Masuda, T.; Takadate, A.; Nakashima, K.; Kuroda, N. *Anal. Chim. Acta* **2010**, *665*, 74−78.

(42) Lee, D. W.; Erigala, V. R.; Dasari, M.; Yu, J. H.; Dickson, R. M.; Murthy, N. *Int. J. Nanomed.* **2008**, *3*, 471−476.

(43) Zhang, X.; Zhou, H.; Ding, C.; Zhang, S. *Chem. Commun.* **2009**, 5624−5626.

(44) Díaz, A. N.; Sánchez, F. G.; González Garcia, J. A. *J. Biolumin. Chemilumin.* **1998**, *13*, 75−84.

(45) Dodeigne, C.; Thunus, L.; Lejeune, R. *Talanta* **2000**, *51*, 415−439.

(46) White, E. H.; Roswell, D. F. *Acc. Chem. Res.* **1970**, *3*, 54−62.

(47) Drew, H. D. K.; Garwood, R. F. *J. Chem. Soc.* **1939**, *0*, 836−837.

(48) Chen, G. N.; Lin, R. E.; Zhuang, H. S.; Zhao, Z. F.; Xu, X. Q.; Zhang, F. *Anal. Chim. Acta* **1998**, *375*, 269−275.

(49) Omote, Y.; Miyake, T.; Ohmori, S.; Sugiyama, N. *Bull. Chem. Soc. Jpn.* **1966**, *39*, 932−935.

(50) Chen, Y.-H.; Yao, W.-Z.; Geng, B.; Ding, Y.-L.; Lu, M.; Zhao, M.-W.; Tang, C.-S. *Chest* **2005**, *128*, 3205−3211.

(51) Hyšpler, R. R.; Tichá, A.; Indrová, M.; Zadák, Z.; Hyšplerová, L.; Gasparič, J.; Churáček, J. *J. Chromatogr., B* **2002**, *770*, 255−259.

(52) Savage, J. C.; Gould, D. H. *J. Chromatogr., B* **1990**, *526*, 540−545.

(53) Wang, R. *FASEB J.* **2002**, *16*, 1792−1798.

(54) Cartwright, I. L.; Hutchinson, D. W.; Armstrong, V. W. *Nucleic Acids Res.* **1976**, *3*, 2331−2340.

(55) Aitken, C. E.; Marshall, R. A.; Puglisi, J. D. *Biophys. J.* **2008**, *94*, 1826−1835.

(56) Jocelyn, P. C. *Eur. J. Biochem.* **1967**, *2*, 327−331.

(57) CLSS-1 and CLSS-2, like other azides, are incompatible with dithiols such as DTT (see ref 54) and phosphine-based reducing agents such as TCEP. For additional examples of this incompatibility, see the Staundinger reaction.

(58) Abushqara, E.; Blum, J. *J. Heterocycl. Chem.* **1990**, *27*, 1197−1200.

(59) Baird, P. D.; Dho, J. C.; Fleet, G. W. J.; Peach, J. M.; Prout, K.; Smith, P. W. *J. Chem. Soc., Perkin Trans. 1* **1987**, 1785−1791.

(60) Darbon, N.; Oddon, Y.; Guy, E.; Ferrari, B.; Pavia, A. A.; Pepe, G.; Reboul, J. P. *Acta Crystallogr., Sect. C: Cryst. Struct. Commun.* **1985**, *41*, 1100−1104.

(61) Tchertanov, L. *Acta Crystallogr., Sect. B: Struct. Sci.* **1999**, *55*, 807−809.

(62) Paradies, H. H. *Ber. Bunsen-Ges. Phys. Chem.* **1992**, *96*, 1027−1035.

(63) Thordarson, P. *Chem. Soc. Rev.* **2011**, *40*, 1305−1323.

(64) CSE produces H_2S five times faster using Hcy as a substrate compared to Cys.

(65) Pfeffer, M.; Ressler, C. *Biochem. Pharmacol.* **1967**, *16*, 2299−2308.

(66) Faccenda, A.; Wang, J.; Mutus, B. *Anal. Chem.* **2012**, *84*, 5243−5249.

(67) Kandil, S.; Brennan, L.; McBean, G. J. *Neurochem. Int.* **2010**, *56*, 611−619.

(68) Allen, C. R.; Richard, P. L.; Ward, A. J.; van de Water, L. G. A.; Masters, A. F.; Maschmeyer, T. *Tetrahedron Lett.* **2006**, *47*, 7367−7370.

(69) Frisch, M. J.; Trucks, G. W.; Schlegel, H. B.; Scuseria, G. E.; Robb, M. A.; Cheeseman, J. R.; Scalmani, G.; Barone, V.; Mennucci, B.; Petersson, G. A.; Nakatsuji, H.; Caricato, M.; Li, X.; Hratchian, H. P.; Izmaylov, A. F.; Bloino, J.; Zheng, G.; Sonnenberg, J. L.; Hada, M.; Ehara, M.; Toyota, K.; Fukuda, R.; Hasegawa, J.; Ishida, M.; Nakajima, T.; Honda, Y.; Kitao, O.; Nakai, H.; Vreven, T.; Montgomery, J. A., Jr.; Peralta, J. E.; Ogliaro, F.; Bearpark, M.; Heyd, J. J.; Brothers, E.; Kudin, K. N.; Staroverov, V. N.; Kobayashi, R.; Normand, J.; Raghavachari, K.; Rendell, A.; Burant, J. C.; Iyengar, S. S.; Tomasi, J.; Cossi, M.; Rega, N.; Millam, J. M.; Klene, M.; Knox, J. E.; Cross, J. B.; Bakken, V.; Adamo, C.; Jaramillo, J.; Gomperts, R.; Stratmann, R. E.; Yazyev, O.; Austin, A. J.; Cammi, R.; Pomelli, C.; Ochterski, J. W.; Martin, R. L.; Morokuma, K.; Zakrzewski, V. G.; Voth, G. A.; Salvador, P.; Dannenberg, J. J.; Dapprich, S.; Daniels, A. D.; Farkas, Ö.; Foresman, J. B.; Ortiz, J. V.; Cioslowski, J.; Fox, D. J. *Gaussian 09, Revision C.01*; Gaussian, Inc., Wallingford, CT, 2009.

(70) Dennington, R.; Keith, T.; Millam, J. *GaussView, Version 5*; Semichem Inc., Shawnee Mission, KS, 2009.

(71) Humphrey, W.; Dalke, A.; Schulten, K. *J. Mol. Graphics Modell.* **1996**, *14*, 33−38.

(72) Ahmad, N.; Maitra, S.; Dutta, B. K.; Ahmad, F. *J. Environ. Sci.* **2009**, *21*, 1735−1740.